11R.6 PRECIPITATION PHYSICS: THE STRUCTURE OF PRECIPITATION AND ITS MODELING IN SPACE AND TIME

GyuWon Lee*[,1], Alan Seed[2], and Isztar Zawadzki[1]

[1]J. S. Marshall Radar Observatory, McGill University, Montreal, Quebec, Canada
[2] Cooperative Research Centre for Catchment Hydrology, Bureau of Meteorology, Melbourne, Victoria, Australia

1. INTRODUCTION

Remote sensing measurements are outcome of the interaction between instrumental characteristics and observed fields. Thus, the quantitative definitions of the measurements are affected by the structure of precipitation fields as well as by the spatial and temporal resolutions. The uncertainty in rain estimates from radar measurements is greatly affected by the spatial and temporal variability of drop size distributions that is responsible for the large stochastic components in an R-Z scatterplot as compared to the deterministic component. We investigate the correlation structure of the stochastic component and its connection to precipitation physics. We model the space-time variability of the stochastic component, to allow the study of the characteristics of remote sensing measurements and various correction techniques (raingage adjustment, attenuation corrections).

2. DATA

The McGill dual-polarization S-band Doppler radar measures radar reflectivity at 5-minute, 1 km resolutions over 24 elevation angles. These volume scan data were used to estimate the radar reflectivity at a constant height of 2 km above sea level, the lowest elevation that is relatively free of ground clutter. Thereafter the data were downscaled to 1-minute, 250 m resolution by sub-sampling the spatial field and using bi-linear interpolation in Lagrangian coordinates to interpolate to the required temporal resolution.

The raindrop size distributions obtained from a Precipitation Occurrence System Sensor (POSS) (Sheppard and Joe 1994) are used to derive the temporal structure of the stochastic components and microphysical parameters. The stochastic model is constrained by this point measurement and is validated with these derived parameters.

The storm of 24 September 2001 was selected as a test case because of the long duration of the rainfall (over 24 hours) and the range of R-Z relationships that were identified during the period. POSS measurements (15 km range and 72 degree azimuth from the radar site) show a total rainfall accumulation of 28 mm and a few peaks in Z and R associated with convective cells. Total rainfall accumulation from POSS Z with a climatological R-Z relationship ($Z = 210R^{1.47}$: Lee and Zawadzki 2005) is similar to the true value since the derived R-Z ($Z = 206R^{1.55}$) for the whole period is quite close to the climatological one. However, the deviation (δ_R) between R and $\bar{R}\,[=(Z/210)^{1/1.47}]$ shows quite interesting features (Fig. 1). For the period from 00 UTC 25 Sept. to 05 UTC 25 Sept 2005, an R-Z relationship is quite similar to the climatological one as indicated by the values δ_R close to zero. The values of δ_R are systematically positive for the next three hours, and negative for the last four hours. Although the derived R-Z relationship for the whole period is quite similar to the climatology, the R-Z relationships for certain periods showed persistent and significant deviation from the mean. The coherence of this deviation can be calculated in terms of the q-th generalized structure function $\gamma(\tau)$ for a given time lag (τ):

$$\gamma(\tau) = \overline{\left[\delta_R(t) - \delta_R(t+\tau)\right]^q} \qquad (1)$$

The calculated second order $\gamma(\tau)$ and autocorrelation $\rho(\tau)$ as a function of time lag (τ) are shown in Fig. 2. The de-correlation time is over one hour and structure function does not become flat. In other words, δ_R does not fluctuate as a white noise process but has coherence over longer periods and this coherence should be considered in the modeling of DSD variability in time and space.

3. Model Description

The objective is to build a statistical model of $\delta_R(\mathbf{x})$, the departures in space and time from a climatological R-Z relationship, excluding the other significant sources of uncertainty. The model must be constructed in such a way that makes it possible to generate stochastic realizations of a rain field that are conditioned on radar reflectivity observations that were downscaled to 1-minute, 250 m resolution.

The model must also describe the fluctuations in space and time in a way that is consistent with the observations, which are limited at present to a time series at a point (POSS measurements). Therefore, assumptions will have to be made regarding the advection of the $\delta_R(\mathbf{x})$ field through the area of interest, the covariance between $\delta_R(\mathbf{x})$ and $Z(\mathbf{x})$, and the structure of $\delta_R(\mathbf{x})$ in space and time. The covariance between $\delta_R(\mathbf{x})$ and $Z(\mathbf{x})$ is assumed to be zero in the interests of simplification and in the absence of evidence to the contrary.

* *Corresponding author address:* GyuWon Lee, J. S. Marshall Radar Observatory, P. O. Box 198, Macdonald Campus, Ste-Anne-de-Bellevue, QC, Canada, H9X 3V9 e-mail: gyuwon.lee@mail.mcgill.ca

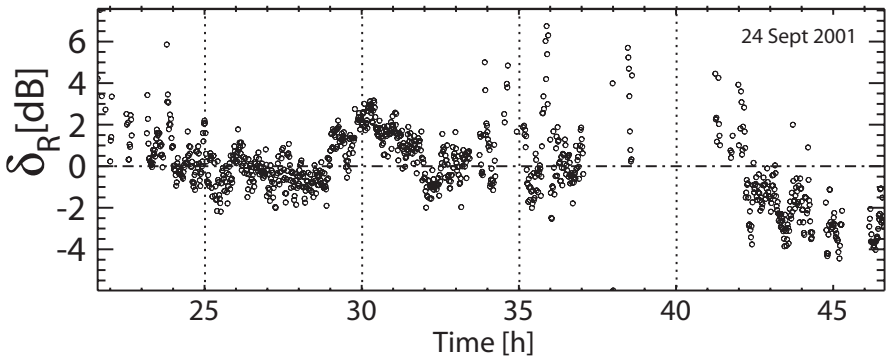

Fig. 1: Time series of δ_R from POSS measurements for the case of 24-25 Sept. 2001. δ_R is defined as $\delta_R[dB] = 10\log_{10}(R) - 10\log_{10}(\widehat{R})$ where $\widehat{R}$ is calculated from Z with a climatological R-Z relationship $Z = 210R^{1.47}$.

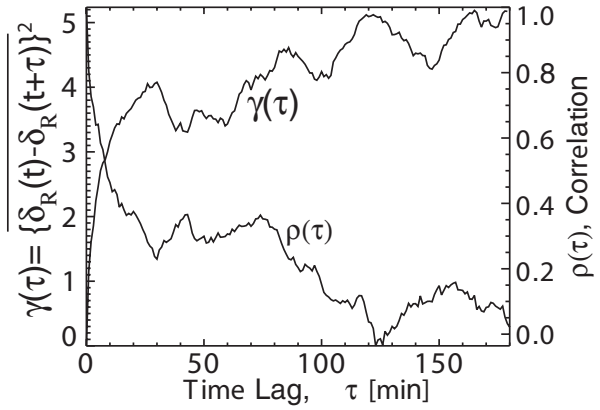

Fig.2: The second order structure function and autocorrelation of $\delta_R[dB]$ as a function of time lag τ. The coherence of structure is over one hour

It seems reasonable to assume that $\delta_R(\mathbf{x})$ and $Z(\mathbf{x})$ are advected together since the physical processes that are driving the perturbations are likely to be embedded in the air mass which is moving at a rate which is similar to that observed in the $Z(\mathbf{x})$ field. Of course this is a simplification and is unlikely to be correct in cases where the apparent motion of $Z(\mathbf{x})$ is due to development and not advection, and in cases where the physical processes are related to the topography under the air mass, which hopefully is stationary. The perturbation field is advected using the velocity field of the observed reflectivity data, which is calculated using the optical flow technique of Bowler *et al*. (2004).

The statistical nature of the time series of the perturbations at a point, $\delta_R(t)$ in Fig. 1 provides some clues regarding the selection of an appropriate model for $\delta_R(\mathbf{x})$. If $\delta_R(t)$ shows strong evidence of a scaling behavior, then a scaling model for $\delta_R(\mathbf{x})$ will be appropriate. POSS data for the 24-25 September 2001 were used to estimate Z and R at 1-minute time steps over a 24-hour period. Thereafter $\delta_R(t)$ was calculated using $\widehat{R} = [Z/210]^{1/1.47}$, the climatological R-Z relationship for Montreal. The power spectrum of the time series of the residuals $\delta_R(t)$ was calculated using the first 1024 data points in the time series, the resulting power spectrum was averaged in octaves as shown in Fig. 3a. The spectrum was found to follow a power law $P \propto f^{-1.04}$, which is consistent with a scaling model (Menabde *et al*. 1997).

The generalized structure function was calculated and was adjusted with the power law model:

$$\gamma(t) = a_0 \tau^{\zeta(q)} \tag{2}$$

that is compatible with the scaling hypothesis. The generalized structure functions for moments 0.4 < q < 2.8 were calculated and the spectra of exponents, $\zeta(q)$, were estimated as shown in Fig. 3b. A straight line fit to $\zeta(q)$ explains approximately 90% of the variance, so a simple self-affine model with a constant scaling exponent can be used to model the time series, at least near the origin and over a limited range of moments.

4. Modelling the R-Z fluctuations in space and time

The scaling nature of $\delta_R(t)$ is quite similar to that displayed by a time series of rainfall at a point so the space-time model developed to model rainfall by Seed et al. (1999) was used to generate $\delta_R(\mathbf{x})$ after the radar measurement model proposed by Jordan et al. (2003).

The space-time model has two components, a model to generate a time series of mean field bias over the domain of the radar reflectivity observations, and a space-time multiplicative cascade to model the small-scale fluctuations about this mean.

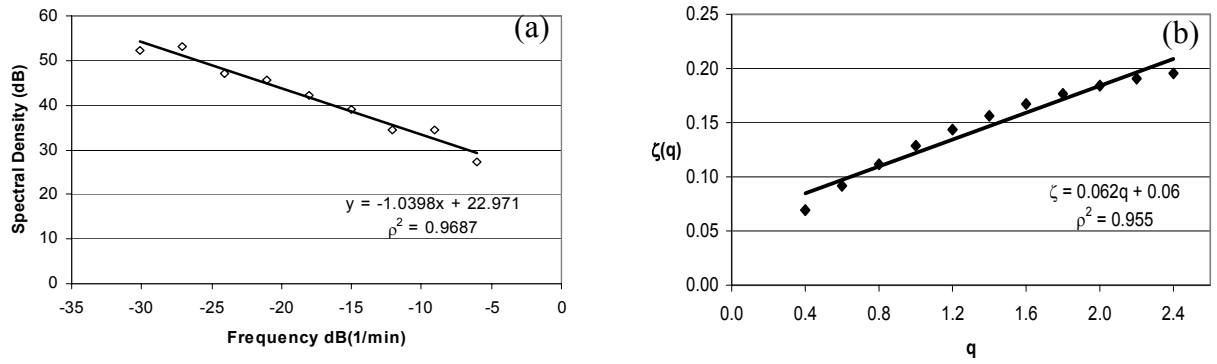

Fig. 3: (a) Spectral density for the time series of $\delta_R(t)$ from POSS measurements for 24 September 2001 with a fitted line (solid line), equation, and determination coefficient (ρ^2). (b) Plot of the exponent of the power law fit to the structure function, $\zeta(q)$, verses the moment of the structure function, q. The fitted line is shown as the solid line with a corresponding equation and determination coefficient (ρ^2).

a. Model of mean field bias

A simple broken-line model results from the linear interpolation between equally spaced independent random variables. Seed *et al*. [2000] developed a multiplicative broken-line model by multiplying *N* simple broken lines together:

$$Z(t) = \prod_{p=1}^{N} \exp\left(\xi_p(t)\right) \tag{3}$$

where $\xi_p(t)$ is the time series from the p^{th} broken line in the cascade.

The variance of each broken line, σ_{Tp}^2, and the spacing between the vertices, a_p, for the p^{th} broken line are given by

$$\sigma_{Tp}^2 = \sigma_{T0}^2 q^{-pH_T}, \qquad a_p = A_0 q^{-p} \tag{4}$$

where σ_{T0}^2 is the variance of the broken line at the outer scale A_0, q is the fractional change in the spacing of the random numbers between successive broken lines, and H_T is the exponent for the change in the variance between successive broken lines in the cascade ($0 < H_T < 1$). This model is able to generate fractional Gaussian noise with a spectral density function that follows a power law.

b. Small-scale model

The model of Seed et al. [1999] was used to generate the space-time fluctuations in the R-Z relationship about the mean field bias. This model uses a multiplicative bounded lognormal cascade model for the spatial distribution and an auto-regressive model for the temporal development in Lagrangian coordinates.

A multiplicative cascade field of size (L_0, L_0) is calculated as the product of *N* fields of correlated random variables where the variance of the k^{th} level, σ_{Sk}^2, is given by

$$\sigma_{Sk}^2 = \sigma_{S0}^2 q^{-2kHs} \tag{5}$$

where q is the ratio of the scales between cascade levels, H_s is the spatial scaling parameter, and σ_{S0}^2 is the variance of the weights at level zero.

The correlation length of the random field at level k, L_k, is given by

$$L_k = L_0 q^{-k} \tag{6}$$

The correlation time in Lagrangian coordinates for level k, τ_{Lk}, is assumed to follow a scaling relationship

$$\tau_{Lk} = \tau_{L0} q^{-kH_{ST}} \tag{7}$$

where H_{ST} is the space-time anisotropy exponent, and τ_{L0} is the Lagrangian lifetime of a structure at spatial scale L_0.

The fields in the cascade are updated in Lagrangian coordinates by means of an auto-regressive lag 2 [AR(2)] model

$$X_{k,i,j}(t+1) = \phi_{k,1} X_{k,i,j}(t) + \phi_{k,2} X_{k,i,j}(t-1) + \delta_k \tag{8}$$

where the model parameters $\phi_{k,1}, \phi_{k,2}$ are functions of τ_k, and the δ_k have a Normal distribution with

$$E[\delta_k] = 0 \tag{9}$$

$$Var(\delta_k) = \frac{1+\phi_{k,2}}{1-\phi_{k,2}}\left[\left(1-\phi_{k,2}\right)^2 - \phi_{k,1}{}^2\right] \tag{10}$$

and spatial correlation length L_k. The cascade levels are advected using the advection field estimated from the radar reflectivity field. The complete list of model parameters is found in Table 1.

5. Case Study

The model was run using the parameters shown in Table 1 and the downscaled radar reflectivity fields. The

model output was verified using the 2nd order structure function of $\delta_R(t)$ evaluated at an area of 25 km by 25 km around the site of the POSS. The temporal generalized structure function was calculated for each pixel in the area and the mean and standard deviation of the structure function was calculated from 10,000 structure functions for each lag out to 120 minutes. The structure function for the POSS together with the mean and standard deviation of the model is shown in Fig. 4a. Estimates of the 2nd order structure function have significant uncertainty, particularly for the longer lag times, but the modeled structure function closely follows the observed structure function for the first thirty minutes. The structure function from POSS is within the standard deviation up to 110 minutes. The mean spectral densities of the input (downscaled) radar rainfall based on the R-Z relationship (thick line) and the model output fields (thin line) are shown in Fig. 4b. The power laws are well preserved in the model (simulation). Spectral density from simulated fields shows larger power than that from downscaled radar Z fields due to the added stochastic components. A slight dip is noticed in the spectral density of both the observed and simulated fields at 1 km resolution. This is due to the loss of variance due to the downscaling procedure.

Table 1: List of model parameters.

Mean dBε	μ	-0.1
Variance at pixel resolution $(dB\varepsilon)^2$	σ^2_{S0}	1.7
Spatial Scaling Exponent	H_s	0.15
Lagrangian Space-Time Exponent	H_{ST}	1.55
Lagrangian Correlation Time (minutes)	τ_{L0}	30
Correlation Time of mean field bias (minutes)	T_0	420
Scaling Exponent of mean field bias	H_T	0.1
Variance of mean field bias $(dB\varepsilon)^2$	σ^2_{T0}	1.25

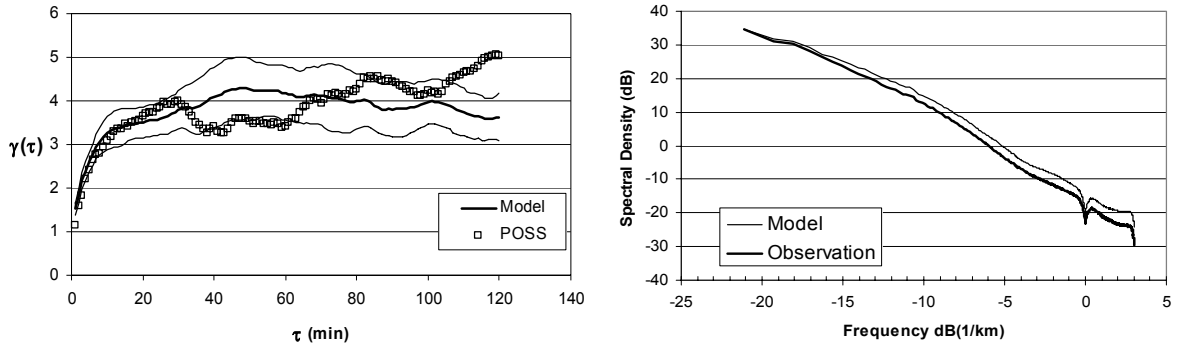

Fig. 4: (a) 2nd order structure functions for the POSS (square) and for the model (thick solid line). The structure function for the model is an average of 10,000 structure functions at an area of 25 km by 25 km around POSS location. The standard deviation is shown as thin lines. (b) Mean spectral density for the input (downscaled) radar and the model (simulated) rainfall fields. The radar reflectivity field was first converted into R using the climatological Z-R relationship and then spectral density was calculated.

Temporal variation of Z, R and $D_m^{'}$ from POSS, radar and, simulation in Fig. 5 shows coherency between measurements and simulation, supporting the validity of the simulation. The characteristics diameter is derived from R and Z (Lee et al 2004). The mean and variance of $D_m^{'}$ from the simulation and POSS measurements are comparable (Table 2). The general trend of $D_m^{'}$ is well simulated although a systematic bias exists due to the difference between radar Z and POSS Z. This is attributed to the fact that the two measurements have different sampling volumes and measurement heights. Since we have simulated only the DSD variability measured from POSS and do not consider the difference between two measurements, a systematic bias does not indicate the failure of the simulation.

Table 2: The mean and variance of $D_m^{'}$ from POSS measurements and model.

	Mean [mm]	Variance [mm^2]
Model	1.29	0.08
POSS	1.34	0.11

Spatial distributions of radar Z and simulated R in Fig. 6 illustrate the effects of adding stochastic components that represent the variability of DSDs. The structure of simulated R and Z fields are similar at the large scale, but the small scale fluctuations are more pronounced in R fields due to the DSD variability. This was indicated in the spectral densities in Fig. 4b which show that the simulated field has more variability at the high frequencies. Fields of drop size distributions can be

calculated given the R and Z fields with a predetermined h(x) that is derived from actual data or a specific DSD model (Lee et al 2004). In addition, two characteristic parameters of DSDs ($N_0^{'}$ and $D_m^{'}$) can be easily obtained from the two fields as shown in Fig. 6. Spatial distribution of $D_m^{'}$ is similar to those of simulated R and radar Z. The correlation coefficients for R-$D_m^{'}$ and Z-$D_m^{'}$ are 0.38 and 0.67, respectively (Table 3). Similar characteristics have been found from POSS measurements. The distribution of $N_0^{'}$ does not show any coherency with R, Z, or $D_m^{'}$ fields (the correlation coefficient is less than 0.2), but the fields do have spatial structure. As shown by Lee et al. (2004), the correlation coefficient between R and $N_0^{'}$ is less than 0.3 whereas $D_m^{'}$ increases with R. Testud et al. (2001) also found the similar trend in convective rain. Thus, our simulation is also quite consistent with their results and POSS measurements.

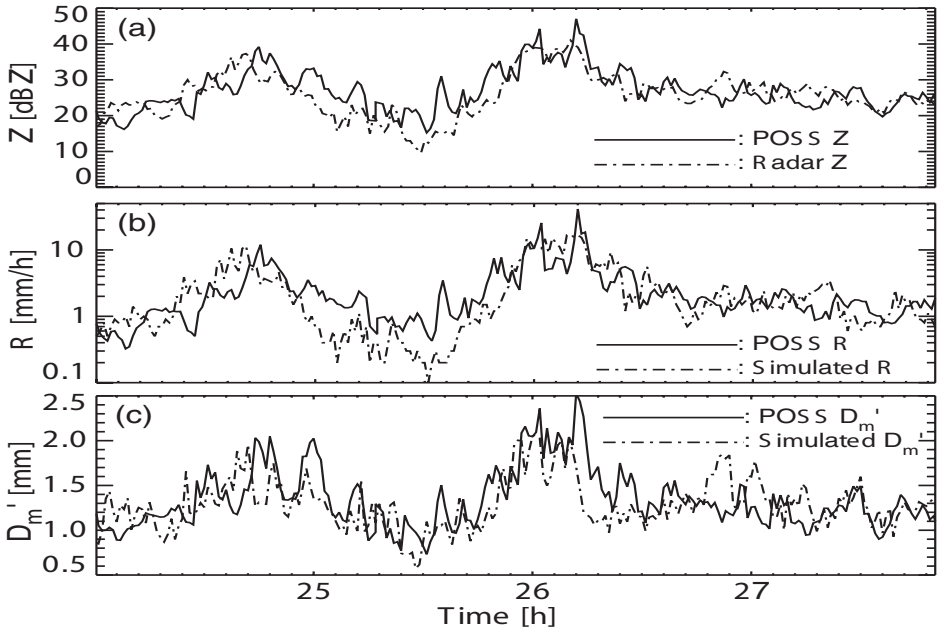

Fig. 5: Time series of Z, R and $D_m^{'}$ from POSS, radar and, simulation.

Table 3: Determination coefficients between DSD parameters.

	$N_0^{'}$ - $D_m^{'}$	$N_0^{'}$-R	$N_0^{'}$-Z	$D_m^{'}$-R	$D_m^{'}$-Z
Model	0.20	0.19	0.02	0.38	0.67
POSS	0.28	0.08	0.00	0.44	0.73

7. Discussion

We have demonstrated a way of constructing fields of the other moment in space and time that are constrained with actual radar and disdrometric measurements at a point. Fields of one moment (Z or 6th moment) of the DSD is obtained from radar measurements and then these reflectivity fields are converted into deterministic R fields. Finally, fields of the other moment (R) are obtained from the combination of the deterministic R fields and stochastic components that are derived from the space-time modeling of the fluctuation with respect to an R-Z relationship. The fluctuations are assumed to be independent of the Z field. The stochastic model is validated at a point by comparing the second order structure functions and characteristic DSD parameters from the model with POSS measurements. The spatial distributions of modeled $D_m^{'}$ are similar to the distributions of radar Z and simulated R whereas $N_0^{'}$ shows completely different distributions. However, $N_0^{'}$ shows the coherent structure in space. In addition, the time series of $D_m^{'}$ from POSS measurements and modeling have similar characteristics, supporting the conclusion that the fields of modeled DSDs are realistic.

With the two fields (radar Z and simulated R fields), the spatial and temporal distribution of DSDs can be derived using the double-moment scaling DSDs (Lee et al 2004). The derived DSD fields can be used as a test bed for many remote sensing techniques: for example attenuation correction techniques, radar-rain gauge adjustments, polarimetric rain estimates, etc. The effect of DSD variability in space and time on radar-rain gauge adjustments can be investigated in a way that the problems of undersampling and drop sorting are fully resolved. In addition, all polarimetric and dual-wavelength parameters, such as differential phase shift, different reflectivity, attenuation, can be easily obtained through a scattering model using derived DSD fields in space and time. With these parameters, several methods of attenuation correction, especially polarimetric attenuation correction, can be tested and

the uncertainty of correction methods can be obtained. In addition, the modeling can incorporate the initial errors in radar quantitative precipitation estimates to investigate their importance in precipitation forecasting systems. This is a comprehensive way of generating an ensemble precipitation forecasting.

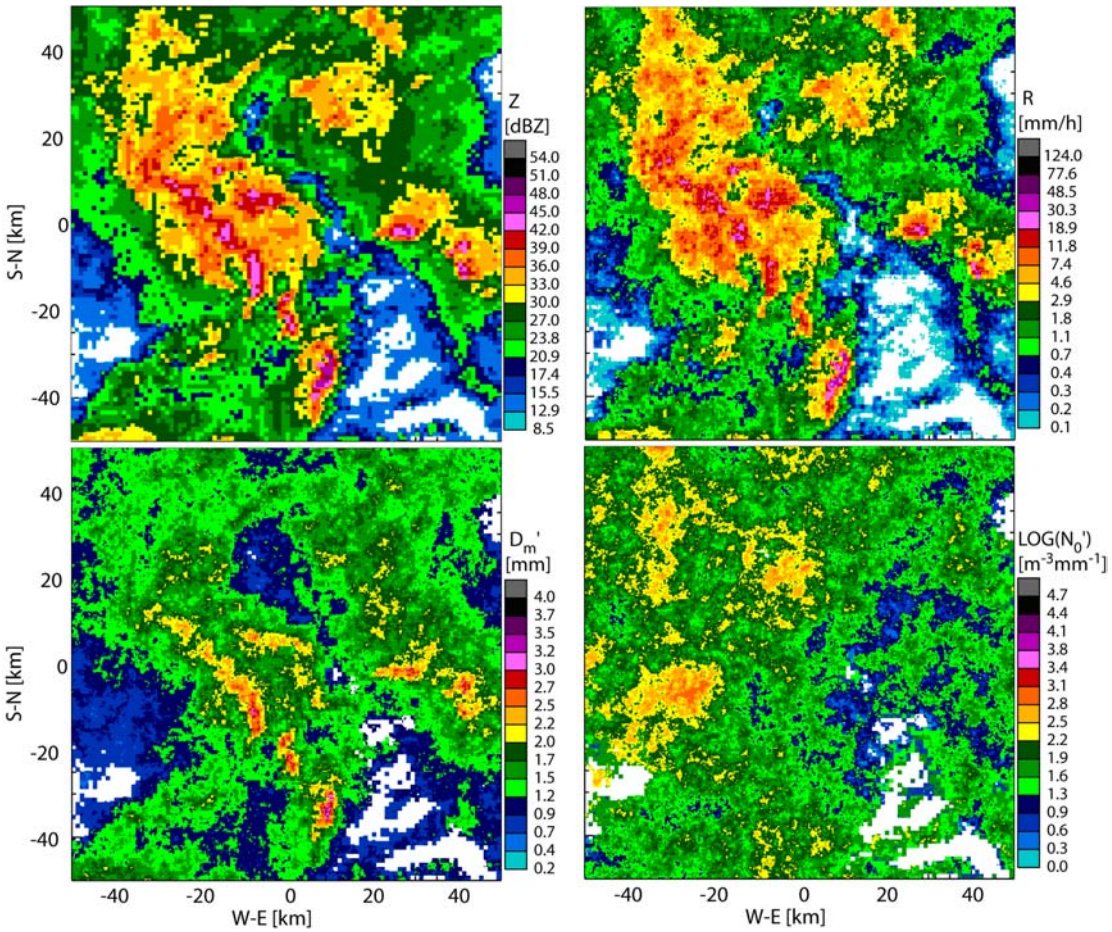

Fig. 6: Spatial distributions of radar Z, simulated R, derived D_m', and N_0' at 01:00 UTC, 25 September, 2001.

References

Bowler, N., C. Pierce, and A.W. Seed, 2004: Development of a precipitation nowcasting algorithm based upon optical flow techniques. *J. Hydrology*, **288**, 74-91.

Jordan, P.W., A.W. Seed, and P.E. Weinmann, 2003: A stochastic model of radar measurement errors in rainfall accumulations at catchment scale. *J. Hydrometeorol*. 841-855.

Lee, G. W. and I. Zawadzki., 2005a: Variability of drop size distributions: Time scale dependence of the variability and its effects on rain estimation. *J. Appl. Meteo.*, **44**, 241-255.

Lee, G. W, I. Zawadzki, W. Szymer, D. Sempere-Torres, and R. Uijlenhoet, 2004: A general approach to double-moment normalization of drop size distributions. *J. Appl. Meteo.*, **43**, 264-281.

Menabde, M., D. Harris, A.W. Seed, G.L. Austin, and C.D. Stow, 1997: Multiscaling properties of rainfall and bounded random cascades. *Water Resour. Res.*, **33**, 2823-2830.

Seed, A.W., R. Srikanthan, and M. Menabde, 1999: A space and time model for design storm rainfall. *J. Geophys. Res.*, **104**, 31623-31630.

Seed, A.W., C. Draper, R. Srikanthan, and M. Menabde, 2000: A multiplicative broken-line model for time series of mean areal rainfall. *Water Resour. Res.*, **36**, 2395-2399.

Sheppard, B. E. and P. I. Joe, 1994: Comparison of raindrop size distribution measurements by a Joss-Waldvogel disdrometer, a PMS 2DG spectrometer, and a POSS Doppler radar. *J. Atmos. Oceanic Technol.*, **11**, 874-887.

Testud, J., S. Oury, R. A. Black, P. Amayenc, and X. Dou, 2001: The concept of "normalized" distribution to describe raindrop spectra: A tool for cloud physics and cloud remote sensing. *J. Appl. Meteor.*, **40**, 1118-1140.